

Finite element modelling of the mitral valve: feasible approaches for understanding the valvular function and evaluating clinical scenarios.

Authors: Emiliano Votta¹, Enrico Caiani¹, Federico Veronesi¹, Monica Soncini¹, Franco Maria ontevecchi², Alberto Redaelli¹

¹ Politecnico di Milano, Bioengineering Department, Milano, Italy

Piazza Leonardo da Vinci 32

20133 Milano, Italy

² Politecnico di Torino, Mechanics Department, Torino, Italy

Corso Duca degli Abruzzi, 24

10129 Torino, Italy

Abstract

Background – In the current scientific literature particular attention is dedicated to the study of the mitral valve and the comprehension of the mechanisms that lead its normal function, as well as of the ones that trigger possible pathologic conditions. One of the adopted approaches consists in computational modelling, which allows the quantitative analysis of the mechanical behaviour of the valve by means of continuum mechanics theory and numerical techniques. However, none of the models currently available in the literature realistically accounts for all of the aspects that characterize the function of the mitral valve.

Aim – In the present study a new computational model of the mitral valve was developed, with the long term aim of applying it to the evaluation of annuloplasty procedures.

Methods – A structural finite element model of the mitral valve was developed taking into account all of the main valvular sub-structures. In particular, the real geometry and the movement of annulus and papillary muscles were reconstructed from 4-D ultrasound data from a healthy human subject. A realistic description of mitral tissues complex mechanical properties was included into the model.

Results – Preliminary simulations show promising results in terms of adherence to reality and quantification of valve biomechanics.

Keywords: Mitral valve, finite element modelling, 3-D ecocardiography

INTRODUCTION

The mitral valve separates the left atrium from the left ventricle and guarantees the unidirectional blood flow from the first to the second chamber. The action of the transvalvular pressure drop, along with the dynamic contraction of the annulus and of the papillary muscles, induces the correct closure and reopening of the valve, as well as its normal interaction with the surrounding ventricular chamber.

The mitral valve is object of particular interest by clinicians, due to the high prevalence of its pathologies that usually have to be surgically treated. In the last two decades clinicians have been searching for increasingly more effective surgical techniques and devices. These, however, need to be carefully designed, tested and optimized prior to being used in the clinical practice. At this purpose different tools and approaches are available, including computer models based on the finite element (FE) method, which allows the numerical solution of the equations of continuum mechanics applied to complex systems. FE modelling is naturally appealing, since it allows the flexible, repeatable and quantitative analysis of multi-factorial scenarios, as the ones that characterize mitral function in pathologic and post-operative conditions. Moreover, FE models, and structural ones in particular, are becoming more and more widely adopted thanks to the continuous increase in computing performance. However, the implementation of a fully realistic FE model of the mitral valve still represents a challenging task, due to the high complexity of the four aspects to be modelled at once: valvular morphology, valvular tissues mechanical response, dynamic loading and boundary conditions during the cardiac cycle and interaction between the mitral valve and surrounding blood.

Only five groups have developed effective three dimensional structural FE models of the human mitral valve, adopting them either to mimic mitral normal function [Kunzelman et al. 1993a, Lim et al. 2005, Prot et al. 2007, Einstein et al. 2005a] or to understand the biomechanics underlying valvular diseases [Kunzelman et al. 1997, 1998a, Einstein et al. 2005b] and surgical corrections [Votta et al. 2001, Maisano et al. 2005, Votta et al. 2007, Dal Pan et al. 2005, Reimink et al. 1995, 1996, Cochran & Kunzelman 1998, Kunzelman et al. 1998b]. Every model was based on simplifying assumptions, whose nature, number and impact varied from model to model, depending on the degree of complexity of the latter and on its particular application. As a result, the four abovementioned aspects were differently accounted for; an overview of the solutions adopted at this purpose is provided in the following paragraphs.

Modelling of Time-Dependent Mitral Morphology

The mitral valve is indeed an apparatus consisting of different substructures, whose correct interaction is necessary to the proper valvular function: the annulus, the two valvular leaflets, the chordae tendineae and

the two papillary muscles (PMs) (Figure 1). A realistic geometrical model of the valve should include all of these sub-structures and should account for their time-dependent shape, proportions and reciprocal positions.

Currently, no one of the published FE models of the mitral valve has this feature. The first general limitation shared by nearly all of the available models consists in assuming reflection symmetry for the entire valve; valve asymmetries were partially accounted for only by Lim and co-workers, who modelled the annulus and the PMs using *in vivo* data [Lim et al. 2005]. The second general limitation shared by the mentioned models consists in the limited timeframe of the simulated phenomenon. None of the mentioned authors simulated the valve function during the whole cardiac cycle; instead, the focus is usually on ventricular systole, the beginning of the simulated phenomenon being end-diastole and its end being either the systolic peak.

The annulus - The first valvular sub-structure is the annulus, which is the boundary of the valve orifice and is in continuity with the surrounding myocardium of the atrium. Its profile is saddle-shaped and changes dynamically during the cardiac cycle [Flachskampf et al. 2000]. When observed from an atrial view, the annulus appears almost elliptical; for this reason its extent is often described in terms of its two main diameters, respectively the septo-lateral and the commissure-commissural one, whose extent changes from diastole to systole [Ormiston et al. 1981, Fyrenius et al. 2001]. In the majority of the models available in the literature the annular profile is defined as an idealized line with a simplified shape, according to geometrical rationales.

The different idealized annular shapes are sketched in the top panel of Figure 2. In particular, Kunzelman and co-workers in their first generation model of physiological mitral valve assumed a planar annulus, which from an atrial view appeared D-shaped and smoothed; the straight part of the D represented the anterior portion of the annulus and the curved tract represented the posterior one [Kunzelman et al. 1993a]. Even though the initial state of the valve was supposed to be the end diastole one, the proportions of the D profile were defined according to the annular typical dimensions in systole and were kept constant through the entire simulation, as if the annulus was akinetic. This annular shape was maintained in the successive versions of the model that were applied to the structural analysis of clinical scenarios [Kunzelman et al. 1997, 1998a, 1998b; Cochran & Kunzelman 1998; Reimink et al. 1995, 1996], as well as in the new generation fluid-structure interaction model recently developed by the same research [Einstein et al. 2005a, 2005b]. Still, the annulus was again assumed flat and akinetic. A similar annular profile was adopted by Dal Pan and co-workers [Dal Pan et al. 2005], who also hypothesised a straight anterior tract of the annulus smoothly connected to an elliptical posterior tract. Annular planarity and lack of contraction characterizes

also the model proposed by Prot and colleagues [Prot et al. 2007] and our first generation model [Votta et al. 2002], where a circular annulus is adopted. A different shape was used in a computational study recently proposed by our research group [Votta et al. 2007]. In this case the physiological profile of the annulus was idealized as the union of two semi-ellipses, which represented the anterior and posterior annulus, with a shared major axis, which represented the valve CC dimension. Still, the overall profile was planar and fixed in time.

The only study that proposed a totally different approach to the modelling of the annulus is the one proposed by Lim and collaborators [Lim et al. 2005]. In their study the authors tracked through time the position of 12 ultrasound crystals implanted on the annulus of a single sheep. Interpolating the markers' position at different time points they were able to define a realistic saddle-shaped, non symmetric annular profile, accounting also for its contraction through the cardiac cycle.

The Leaflets - The second fundamental valvular substructure consists of the two leaflets, named respectively anterior and posterior, which are distinct from a functional point of view although they form a single membranous structure inserted onto the annulus (Figure 1). The first one consists of a single wide cusp, is inserted on a shorter tract of the annulus but is more extended in the annulus-to-free edge direction. The second one has three cusps, is inserted on a longer tract of the annulus but it is shorter in the annulus-to-free edge direction. Both leaflets have a non-constant thickness, being thicker in the annular and commissural regions and thinner in the belly region. Leaflets extent and morphology were quantitatively characterized by experimental measurements on fresh human and porcine valves, the two populations having been proved to be not statistically different [Kunzelman et al. 1994]. However, these were converted into a leaflet geometrical model with different approaches, which are sketched in the bottom panel of Figure 2. The simplest approach to the geometrical modelling of mitral leaflets was adopted by Lim and colleagues [Lim et al. 2005], who described them as a single membrane, with a constant 1.26 mm thickness, that, in the open valve configuration, lies on a nearly conical surface that originates from the annulus profile and whose free margin does not have any cusps. Thus, the local morphological details that characterize the leaflets are neglected. In all of the other models the anterior and posterior leaflets are described as two different entities, each one with its own geometrical features. In the model proposed by Prot and co-workers [Prot et al. 2007], as well as in the ones developed by Dal Pan and colleagues and by Kunzelman's research group [Kunzelman et al. 1993a, Einstein et al. 2005a], each leaflet is defined as a single cusp. However, these models differ because of some details: the initial position of the leaflets, their thickness and the description of their commissural region. In the Prot's model, the valve in its initial condition is totally open, the leaflets,

assumed uniform and equal to 1 mm, are inserted on completely opposite sides of the annulus, so that the commissural region is not modelled. In the Dal Pan's model, the valve in its unloaded configuration is assumed almost closed, the leaflets being separated by a small gap. The commissures are modelled as a pair of hinges, where the leaflets free edge converge, rather than an actual part of the leaflets. In Kunzelman's model, the valve in its initial condition is not totally open and the leaflets form an entire membranous structure, which includes the two commissural regions. Moreover, thickness varies depending on the model leaflets region. A different solution was adopted in the models we developed in the past, where the valve was assumed initially totally open, i.e. the leaflets were assumed laying on a cylindrical surface whose generatrix was the annulus. Moreover, the three cusps usually observable in the posterior leaflet were explicitly accounted for and a constant thickness of 0.8 mm was assumed.

Chordae Tendineae and Papillary Muscles - The last mitral structures to be considered are chordae tendineae and PMs, which are often referred to as the sub-valvular apparatus. Chordae tendineae are branched fibrous strings that connect the leaflets to two PMs, which protrude from the left ventricular wall and are named, respectively, antero-lateral and postero-medial (Figure 1). Chordae tendineae are commonly classified as marginal, basal and strut, according to the respective insertion zone on the leaflets. These are, respectively, the leaflets free margin, the annular region of the posterior leaflet and the belly of the anterior one. As demonstrated by published experimental studies, different chordae types have different functions. Marginal chordae, which are stiffer and thinner, bare the main part of the pressure loads acting on the valve, while basal and strut chordae regulate the dynamics of valve closure [Obadia et al., 1997; Timek et al., 2001; Goetz et al., 2003]. The PMs consist of one or more conical tips, where chordae depart from, that originate from a main almost globular core. These two muscles move and contract synergically with the ventricular myocardium during the systolic phase, in order to stretch chordae tendineae and thus prevent mitral leaflets from prolapsing into the atrium.

As far as chordae tendineae are concerned, the most common simplifications consist in neglecting their branched structure and in accounting only for the presence of marginal chordae, which, according to experimental findings, bare the major portion of the pressure load that closes the valve during ventricular systole. These assumptions are present in the first generation structural model by Kunzelman's research group [Kunzelman et al. 1993], in the studies we performed in the past years [Votta et al. 2002, Maisano et al. 2005, Votta et al. 2007], in the one by Prot and colleagues [Prot et al. 2007] and in the model adopted by Dal Pan et al. [Dal Pan et al. 2005], who also verified that the action of marginal chordae can be implicitly accounted for by imposing proper kinematical boundary conditions to the leaflets free margin. As for other

modelling aspects, the most sophisticated approach was adopted by Einstein and colleagues [Einstein et al. 2005a, 2005b], who accounted for the presence of all types of chordae, marginal, basal and strut, as well as for their branched insertions into the leaflets.

As far as PMs are concerned, they are never modelled as anatomical entities with finite dimensions and physical properties. Instead, their tips are usually included into the model as the origins of chordae tendineae; their movement can be imposed to simulate the effect of PMs contraction during the cardiac cycle. The only study that accurately defined the position and the movement of PMs tips is the one by Lim and colleagues [Lim et al. 2005], who used animal in vivo data also to implement this aspect of the model. Papillary muscles contraction was also modelled by Kunzelman and colleagues in their second generation structural model, but in a more idealized fashion; their pulling action was simulated by displacing them 1 mm away from the valve orifice, towards the ventricular apex. In all of the other models herein discussed the initial PMs position is set following geometrical criteria that, although rational and consistent, provide an idealized description. Moreover, their time-dependent movement is neglected.

Modelling of Tissues Mechanical Response

The tissues of the mitral valve sub-structures are soft and hydrated. Their stress-strain response is the macroscopic result of their microscopic inner structure. Usually the annulus and the PMs, although being proper anatomical entities with their own mechanical properties, are treated simply as the boundary between the mitral valve and the surrounding ventricular wall, which boundary conditions can be applied to. For this reason, the physical properties of these sub-structures are normally neglected. On the other hand, the description of the physical properties of mitral leaflets and chordae tendineae has always been considered a key-aspect in mitral valve FE modelling.

The Leaflets - Mitral leaflets tissue might be described as a multi-layer, fibre-reinforced material, whose main constituents are water, collagen, elastin and glycosaminoglycans [Kunzelman et al. 1993]. Among them, collagen and elastin play a pivotal role and determine the biomechanical behaviour of the leaflets tissue; collagen fibres, crimped when the tissue is unloaded, are preferentially oriented parallel to the annulus when the leaflets' belly is considered, independently from the examined tissue layer [Kunzelman et al. 1993b, May-Newman & Yin 1995]. This structure confers to the leaflets a non-linear and transversely isotropic mechanical response, the direction of the collagen fibres being the one with a different stress-strain behaviour as compared to all of the other ones. Moreover, the amount of collagen fibres embedded in the

elastic matrix is higher in the anterior leaflet and lower in the posterior one, the latter being thus more extensible.

Currently only two models include a realistic description of leaflets stress-strain behaviour: the structural one by Prot and colleagues [Prot et al. 2007] and the fluid structure interaction one by Einstein and collaborators [Einstein et al. 2005a]. In both cases the stress-strain relationship is modelled by means of a strain energy function Ψ , accordingly with the theory of hyperelasticity. In general, Ψ is a function of the components of the strain tensor and its derivatives allow the calculation of the corresponding component of the stress tensor.

Prot and colleagues [Prot et al. 2007] adopted two functional forms of Ψ . The first one was initially proposed by May-Newman and Yin [May-Newman & Yin 1995] and is written as follows:

$$\Psi(I_1, I_4) = c_0 \left[e^{c_1(I_1-3)^2 + c_2(\sqrt{I_4}-1)^2} - 1 \right]$$

Where c_i , $i=0, 1, 2$ are the material constitutive parameters. I_1 is the first invariant of the right Cauchy-Green strain tensor \mathbf{C} and I_4 is its fourth invariant, defined as $I_4 = \mathbf{a}_0 \cdot \mathbf{a}_0$, \mathbf{a}_0 being the vector that identifies the fibres collagen fibres direction within the leaflets tissue in its unloaded configuration. The quantity $(\sqrt{I_4} - 1)^2$ accounts for collagen fibres response to traction and is considered only when $I_4 \geq 1$, i.e. when collagen fibres are stretched. The second and alternative functional form is:

$$\Psi(I_1, I_4) = c_0 \left[e^{c_1(I_1-3)^2 + c_2(I_4-1)^2} - 1 \right]$$

Where the indicated parameters have the same meaning they have in the previous strain energy function. Both functional forms allow to realistically reproduce the stress-strain behaviour exhibited by mitral leaflets in experimental traction tests and both of them guarantee, from a theoretical point of view, the mechanical stability of the modelled material. However, according to the authors, the second form was computed more efficiently once it had been implemented by means of a UMAT used defined material subroutine to be included into their model developed by means of the ABAQUS/Standard software.

Einstein and collaborators [Einstein et al. 2005a] adopted a different strain energy function, based on the actual microstructure of leaflets tissue, following the approach previously proposed by Billiar and Sacks to characterize the mechanical properties of aortic valve cusps [Billiar & Sacks 2000]. In this case, the second Piola-Kirchoff stress tensor \mathbf{S} is calculated according to the following mathematical relationships:

$$\mathbf{S} = p\mathbf{J}\mathbf{C}^{-1} + 2\mathbf{J}^{-2/3}\text{DEV} \left[\frac{\partial \tilde{W}}{\partial \tilde{\mathbf{C}}} \right]$$

$$\frac{\partial \tilde{W}}{\partial \tilde{\mathbf{C}}} = \alpha \mathbf{I} + \int_{-\pi/2}^{\pi/2} S_f R(\vartheta) \mathbf{A} \otimes \text{Ad} \vartheta$$

$$= \alpha \left\{ \left[\frac{\beta}{\sigma} (\vartheta) (\vartheta)^{-1} \right] \right\}$$

$$R(\vartheta) = \frac{1}{\sigma \sqrt{2\pi}} \exp \left[-\frac{(\vartheta - \mu)^2}{2\sigma^2} \right]$$

where \mathbf{C} is the right Cauchy-Green strain tensor, J its Jacobian and p the hydrostatic pressure; S_f is the function that describes collagen stress-strain behaviour, \mathbf{I} the identity matrix, \mathbf{A} the orientation tensor; α and β are material's constitutive parameters and $R(\theta)$ accounts for the statistical normal distribution of fibers, which are rotated, as an average, by an angle μ with respect to a fixed direction in space, σ being the standard deviation of their orientation.

All of the other models available in the literature adopt simpler approaches, neglecting different aspects of leaflets mechanical properties depending on the particular model. Dal Pan and colleagues neglected leaflets anisotropy and differences between the two mitral leaflets. However, in order to assess the impact of neglecting also non-linearities, compared two different constitutive models: a linear one, characterized by a Young modulus of 4 MPa and a Poisson ratio of 0.45 to model the leaflets nearly incompressible behaviour, and a hyperelastic one, consisting in a fifth-order reduced polynomial form whose constitutive parameters were set accordingly with experimental results [Dal Pan et al. 2005]. The comparison pointed out that accounting for the non-linear response of the leaflets leads to much lower values in the estimation of leaflets stresses. On the other hand, in the structural models developed by Kunzelman's research group [Kunzelman et al. 1993 and following] and by our research group [Votta et al. 2002, Maisano et al. 2005, Votta et al. 2007] leaflets non linear response was neglected and their anisotropy was accounted for. In both cases a 0.488 Poisson ratio was assumed to model the nearly incompressible behaviour of the tissue, the Young modulus of the anterior leaflet was assumed equal to 6.23 and 2.08 MPa in the direction parallel and perpendicular to the annulus, respectively, and the corresponding values set for the posterior leaflet were 2.35 and 1.88 MPa. All values resembled the tangent elastic modulus exhibited by mitral leaflets for large strains, when all collagen fibres within the tissue are recruited. The simplest modelling of leaflets mechanical response was used by Lim et al. [Lim et al. 2005], who neglected differences between the two leaflets and assumed them to be of linear and isotropic material, with a Young modulus of 0.8 MPa, this value being particularly low with respect to the others adopted in the literature, and a 0.45 Poisson ratio.

Chordae Tendineae – Chordae tendineae essential framework is constituted by a crimped collagen fibres central core recovered by elastic fibres and both enveloped by endothelium [Millington-Sanders et al. 1998]. This micro-structure provides the mechanical response that is typical of collagenous tissues. This response is non linear and characterized by a relatively low Young modulus at small strains and by a high Young modulus at large strains, with a transition region at intermediate strain values. From a mathematical point of view hyperelasticity is a suitable theory to describe this behaviour and was adopted by Einstein, Prot and us [Einstein et al. 2005a, Prot et al. 2007, Votta et al. 2007]. In the first generation structural model by Kunzelman's research group [Kunzelman et al. 1993], as well as in the one by Lim and colleagues [Lim et al. 2005], a simpler linear elastic stress-strain response was modelled. However, while in the first case a Young modulus of 40 MPa and 22 MPa was adopted for marginal and basal or strut chordae, in the second case a stiffer behaviour was hypothesised, with a 132 MPa Young modulus. The simplest modelling solution was adopted by Dal Pan and co-workers [Dal Pan et al. 2005], who described chordae tendineae as inextensible, that is rigid.

Moreover, since chordae are structured as strings, they only resist to traction loads and yield to compressive ones. To account for this feature Einstein [Einstein et al. 2005a] and Lim [Lim et al. 2005] used traction-only elements available in the code they adopted to implement their respective models. A different solution was adopted in our most recent model [Votta et al. 2007], where each chordae was discretised into several elements, thus resulting in a structure that immediately yields to compressive loads.

Loading Conditions

Lim and colleagues [Lim et al. 2005] simulated the mitral function throughout the entire cardiac cycle. Thus, in order to account for the effects of the trans-valvular pressure drop acting on the leaflets, they applied the real atrial and ventricular time-dependent pressures on the corresponding sides of the leaflets. All of the other models cited so far focused their analysis on mitral valve closure from end diastole to the systolic peak. In the structural models leaflets are loaded directly by a time-dependent pressure load, usually according to idealized pressure curves, while in the case of the Einstein's fluid-structure interaction model pressure on the leaflets is a consequence of the fluid-dynamics within the fluid domain, thus being more realistically modelled.

Valve-Blood Interaction

The fluid-structure interaction between mitral leaflets and the surrounding blood was taken into account only by Einstein and colleagues [Einstein et al. 2005a], who immersed the modelled valve into a regular fluid domain that resembles possible in vitro conditions to be used as validation benchmark rather than the actual heart chambers.

A POSSIBLE NEW MODELLING STRATEGY

The overview of the approaches adopted to model the mitral valve shows that none of the cited research groups has been able to realistically model all of the key aspects of the mitral function, not even in the most sophisticated study [Einstein et al. 2005a, 2005b]. The latter describes accurately the leaflets and chordae tendineae morphology, accounts tissues' non linear and anisotropic mechanical response and includes the fluid-structure interaction between the valve and the surrounding blood. However, it does not account for the real annular profile nor for its natural dynamics during the simulated period of the cardiac cycle, i.e. in the timeframe from end diastole to the systolic peak. Moreover, it does not simulate the movement of PMs tips.

In the present study we propose a different modelling approach, which is clinically driven and aimed in particular at the analysis of the effects of different annuloplasty procedures performed to correct mitral insufficiency. For this particular application, it is fundamental to correctly model the annulus initial geometry and its dynamics during the simulated phenomenon. Thus, we developed a new structural FE model that takes into account all of the main valvular sub-structures, includes a realistic description of the physical properties of the respective tissues and comprises an accurate description of initial geometry and dynamics of the annulus and PMs, based on 4-D (3-D volume during time) ultrasound data from human subjects. Thus, when compared to the fluid structure interaction model developed by Kunzelman's research group [Einstein et al. 2005a, 2005b], the approach herein proposed lacks of a key-aspect, fluid-structure interaction, but includes an extra important feature; realistic kinematical boundary conditions based on in vivo data. As a first preliminary benchmark to test the modelling strategy, the closure of a healthy mitral valve, from end diastole to the systolic peak, was simulated. Finite element simulations were run using the ABAQUS/Explicit commercial software, version 6.7-1 (SIMULIA).

Reconstruction of the initial valve geometry from ultrasound data

The end diastole valve configuration was chosen as the initial, unloaded one, since at this point in time the trans-valvular pressure drop acting on the leaflets is almost zero. The reconstruction of the valve geometry, depicted in Figure 3a, was performed through a semi-automatic procedure consisting of three consecutive

steps. These correspond to the reconstruction i) of annulus and PMs, ii) of the leaflets and iii) of chordae tendineae, respectively.

Annulus and Papillary Muscles - Transthoracic real-time 3D echocardiography (RT3DE, Philips) was performed on a healthy subject. The acquired data, characterized by a 31 Hz time frequency, were processed using new in-home custom software for the mitral annulus frame by frame tracking on 3D ultrasound datasets [Veronesi et al. 2007]. In the end diastole frame, which corresponded to the beginning of the QRS complex in the subject's ECG, 36 points were manually selected on the annulus and a further point was selected on each visible tip of the two PMs, as exemplified in Figures 3b and 3c. The 36 points on the annulus were interpolated three dimensionally with 6th order Fourier functions to obtain a continuous annular profile. The latter was then sampled into 404 equally spaced points, which represented the seeding for the leaflets discretized geometry.

As far as PMs are concerned, a single point was defined as the centre of mass of the corresponding selected tips, thus obtaining a single tip for each muscle.

Leaflets – leaflets geometrical model was generated accordingly with anatomical measurements reported by Kunzelman and co-workers [Kunzelman et al. 1994]; it includes both leaflets, the posterior one having three cusps, and the commissural regions. As in our previous models [Votta et al. 2002, Maisano et al. 2005, Votta et al. 2007], a sinusoidal function was used to describe the annulus-to-free margin extent of the leaflets. The function, whose coefficients were originally chosen to suit a valve with an 88 mm long annulus, was scaled consistently with the length of the reconstructed annulus.

Leaflets were originally generated by extruding the annulus along the z-axis, i.e. perpendicularly to the annular plane, and then tilted at their insertion on the annulus in order to reproduce their end diastole position as provided by echocardiographic data (Figure 3d); for the particular simulated subject, the anterior leaflet was tilted by 8.3° with respect to a plane parallel to the z-axis, while the posterior one was tilted by 5.3°. The anterior and posterior leaflets were assumed 1.32 mm and 1.26 mm thick, respectively, and were discretized by means of 48480 three-nodes shell elements with reduced integration.

Chordae – 58 marginal and 2 strut chordae were included into the model, while basal chordae were neglected. Chordae were modelled as straight strings without branches, originating from the two PMs. For this reason the amount of modelled chordae resembled the one of chordae insertions into the leaflets. A cross sectional section of 0.4 and 2.05 mm² was assumed for marginal and strut chordae, respectively.

Reconstruction of kinematical boundary conditions from ultrasound data

The 36 points selected on the annulus at end diastole were automatically tracked throughout the cardiac cycle, so that their positions in time were available. As done for the coordinates obtained at end diastole, the coordinates referred to every point in time were translated and rotated in order to be expressed in a proper cylindrical coordinate system. They were then interpolated and sampled in 404 equally spaced points, whose time-dependent positions were used to calculate the corresponding time-dependent displacements to be used as kinematical boundary conditions within the simulation. The displacement calculation was carried out removing those contributions whose only consequence consisted in rigid motions of the entire valvular apparatus.

Papillary muscles positions through time, and consequently their displacement through time, were not available; because of the four chambers view adopted in the echocardiographic acquisition it was not possible to automatically track them. Thus, once their position at end diastole was known, a geometrical criterion was adopted to estimate their position in the following time points. On the basis of the experimental observations of Dagum and co-workers [Dagum et al. 2000], at end diastole their distances from the trigones, the commissures and the mid-point of the posterior annulus were calculated. At every point in time the position of PMs was looked for as the one that preserved the calculated distances.

Tissues Mechanical Properties

Leaflets stress-strain response was modelled as elastic, non-linear, transversely isotropic and isochoric. At this purpose we adopted the strain energy function suggested by Prot and colleagues [Prot et al. 2007], whose polyconvexity and thermodynamic stability are guaranteed. The strain energy as a function of the strain tensor is hence defined as:

$$\psi(I_1, I_4) = c_0 \left[e^{c_1(I_1-3)^2 + c_2(I_4-1)^2} - 1 \right]$$

Where c_i , $i = 0, 1, 2$ are the material constitutive parameters and are equal to 0.052 kPa, 4.63 and 22.6, respectively, for the anterior leaflet and 0.171 kPa, 5.28 and 6.46 for the posterior one. I_1 is the first invariant of the right Cauchy-Green strain tensor and I_4 is its fourth invariant, defined as $I_4 = a_0 C a_0$, a_0 being the vector that identifies the fibres collagen fibres direction within the leaflets tissue in its unloaded configuration.

The quantity $(I_4 - 1)^2$ accounts for collagen fibres response to traction and is considered only when $I_4 \geq 1$, i.e. when collagen fibres are stretched.

The reported strain energy function was included into the FE model via a VUMAT subroutine implemented in fortran90 and interfaced with the explicit solver used in the simulation.

Chordae tendineae mechanical response was described as elastic, non linear and isotropic by means of a second order polynomial strain energy function, which is available in the hyperelastic materials library within the ABAQUS software. The constitutive coefficients to be used in the characterization of marginal and strut chordae response were calculated by interpolating experimental data from the literature [Kunzelmann et al. 1990].

External Loads

The pressure drop acting on mitral leaflets was modelled as a pressure load applied to leaflets ventricular surface. The load increased up to a systolic peak value of 120 mmHg, with a time-dependency already adopted by other authors [Prot et al. 2007]. The time-scale of the simulated event was scaled: in vivo it lasts for about 0.15 s, while in the simulation the systolic peak was reached in 1 s. This choice allowed avoiding extremely abrupt contact phenomena and obtaining convergence more easily.

Contact Interactions

Contact between the leaflets was accounted for by means of the general contact algorithm available in ABAQUS. As in our most recent FE study [Votta et al. 2007], a friction coefficient equal to 0.05 was assumed to describe leaflets interaction tangentially to their contact surface. Penalty contact was used to describe leaflets mechanical interaction in the direction normal to their contact surface.

Preliminary Simulations Results

Leaflets deformation and coaptation during valve closure are depicted in Figure 4, where the atrial view of the valve is depicted six subsequent frames from end diastole to the systolic peak. Even from this qualitative pictures three outcomes are evident. The first one consists in the change in annular profile from frame to frame, which is visible even in an atrial view. The second one regards the asymmetry of the deformed configurations of the valve; the two lateral cusps of the posterior leaflet (normally called P1 and P3 in the clinical practice) are differently deformed.

The third outcome relies in the fact that coaptation occurs at very low values of trans-valvular pressure drop (when a 16 mmHg value is reached the valve orifice is already occluded) and that after the trans-valvular pressure drop reaches 68 mmHg the valve undergoes only minor further deformations, which are mostly

associated to the motion of annulus and PMs and to the development of deeper wrinkles at the commissures and paracommissures. This outcome is consistent with the leaflets mechanical response; due to their non linear behaviour they undergo large deformations and thus coapt even for a small pressure applied to the leaflets. Once a threshold strain value is reached (about 0.20), which corresponds to the complete recruitment of the collagen fibres embedded in their tissue, leaflets stiffen and a further increase in the applied pressure does not cause major further deformations.

The distribution of maximum principal stresses acting on the leaflets for increasing values of the trans-valvular pressure drop is reported in Figure 5. The comparison of the corresponding contour plots provides two main indications. First, as reasonably expected the most stressed regions are the ones close to chordae insertions, either of marginal or strut ones. This general pattern is observed both in the antero-lateral and in the postero-medial halves of the leaflet; however, in the latter peak stress areas are more extended. Second, while the valve geometrical configuration does not change greatly after leaflets coaptation, the peak stress values follow a different trend. Consistently with leaflets stiffening at large strains, stresses increase more and more rapidly as the pressure load on the leaflets increased. In particular, for a trans-valvular pressure drop of 80 mmHg ($t=0.025$ s) the stress peak value is about 800 kPa and occurred at the insertion of strut chordae. The belly of the anterior leaflet undergoes stresses that range from 60 to 400 kPa. The posterior leaflet experiences lower stress value, in the order of 60 kPa, the central cusp being the most stressed one. When the systolic peak pressure (120 mmHg) is applied to the leaflet, the peak stress reaches 1200 kPa. Stresses acting on the belly of the anterior leaflet range from 130 to 540 kPa, while the ones acting on the posterior one are, again, lower (60÷270 kPa).

Marginal and structural chordae tensions were also calculated. At the systolic peak the majority of marginal chordae experience tensions ranging from 0.11 to 0.28 N, even though a peak value of 0.41 N was detected in the chordae inserted in the paracommissures. Strut chordae response reflected the model's asymmetry; the chord originating from the antero-lateral PM bares a 1.31 N load, while the one originating from the postero-medial PM bares a 2.26 N tension.

Reaction forces at the two nodes representing the PMs were calculated. Their evolution through time resembles the one of the pressure applied to the leaflets; a rather steep increase occurs in the early part of valve closure, while in its final one a plateau is reached. The final and maximum force value, obtained for a trans-mitral pressure drop of 120 mmHg, is 6.24 N for the antero-lateral PM and 6.79 N for the postero-medial one. After 260 ms from end diastole, when an 80 mmHg pressure is applied to the leaflets, these values are 3.98 and 3.91 N, respectively.

Comments

We presented here a structural FE of the mitral valve that combines a detailed description of valvular geometry and tissues mechanical response with the modelling of annular real contraction and PMs movement on the basis of in vivo data from a human healthy subject. To the authors' knowledge, this is the first time that these features are comprised in a single FE model all together.

The preliminary simulation performed on the model provided promising results. Even though the model may undergo future refinements, discussed more in detail in the next section, and even if it needs further testing, some of the indications it provided may be discussed.

In particular, the calculated stress pattern, when compared to the one reported by Einstein and colleagues [Einstein et al. 2005a] is somewhat similar when similar pressure loads are considered. Still, stress values are here higher, the main difference being noted in the case of the peak values. These differences may be due to several factors. Possibly, one of them relies in the different initial valve geometry. In the present study the two leaflets are more far away from each other; in order to coapt they undergo larger deformations and, thus, larger stresses. A further reason is probably in the different modelling of the chordal apparatus: Einstein and colleagues included also basal chordae in their model and this morphological detail may have allowed obtaining a different load transfer from chordae tendineae to mitral leaflets.

As far as chordae tendineae tension is concerned, the calculated values are comparable with the ones gathered in vitro, on 6 human mitral valves, by Jimenez and colleagues [Jimenez et al. 2005], who measured a 1.11 ± 0.57 N load on strut chordae, a 0.18 ± 0.16 N load on anterior marginal chordae and a 0.08 ± 0.11 N load on anterior marginal ones.

With reference to PMs reaction forces, the values of 3.98 and 3.91 N for the antero-lateral and postero-medial PMs, calculated for a 80 mmHg pressure drop across the valve, are greater than the 2.5 N calculated by Einstein's model and observed in previous in vitro studies [Jensen et al. 2001, Hashim et al. 1997] for the same pressure drop value. However, this difference could be due to the contraction of PMs simulated in the present preliminary study, which is not accounted for in the mentioned studies. The displacement imposed to PMs may cause an extra stretch to chordae tendineae, as compared to the one associated to a fixed PMs condition. Thus, PMs should exert an extra traction load to maintain the system's dynamic equilibrium.

Current Limitations and Future Developments

The model, in its current version, represents the benchmark to test the reliability of a new modelling approach that will be further developed to become an optimal tool for the evaluation of annuloplasty procedures. At this purpose, some current limitations will be overcome in the future. These regard first of all the modelling of chordae tendineae; basal chordae should be added to the model and a more realistic, branched structure should be used to describe single chordae. In the authors' opinion, this future improvement may modify the calculated leaflets stress pattern, since chordae tension would be transmitted to the leaflets in different areas and, as an overall, in a more distributed fashion.

A second limitation of the model consists in the assumption of constant thickness within each leaflet. This limitation could be overcome by using, for instance, the thickness pattern reported by Kunzelman in a recent publication concerning her research group's FSI model [Kunzelman et al. 2007].

Moreover, since the modelling of a healthy valve is a benchmark to test whether the model is able to reliably reproduce the valvular function, the method should be validated and its robustness tested prior to being applied for its final goal, i.e. the evaluation of post-operative scenarios associated to annuloplasty procedures and, on the long run, the possible use of this approach as a predictive tool. At this purpose, the method should be extended to the modelling of more healthy valves and for every case its results should be compared with experimental measurements gathered from the literature or by means of proper *in vitro* models. A further interesting, even if semi-quantitative, validation method could consist in comparing the valve dynamics provided by FE modelling to the one reconstructed directly through real time 3D trans-thoracic echocardiography.

References

- Billiar KL, Sacks MS. 2000 Biaxial mechanical properties of the native and glutaraldehyde-treated aortic valve cusp: Part II – A structural constitutive model. *J. Biomech. Eng.* **122**:327-335.
- Cochran RP, Kunzelman KS. 1998 Effect of papillary muscle position on mitral valve function: relationship to homografts. *Ann. Thorac. Surg.* **66**(6 Suppl):S155-61.
- Dagum P, Timek TA, Green GR, Lai D, Daughters GT, Liang DH, Hayase M, Ingels NB Jr, Miller DC. 2000 Coordinate free analysis of mitral valve dynamics in normal and ischemic hearts. *Circulation* **102**[III]:III62-III69.
- Dal Pan F, Donzella G, Fucci C, Schreiber M. 2005 Structural effects of an innovative surgical technique to repair heart valve defects. *J. Biomech.* **38**:2460-2471.

- Einstein DR, Kunzelman KS, Reinhall PG, Nicosia MA, Cochran RP. 2005a Non-linear fluid-coupled computational model of the mitral valve. *J. Heart Valve Dis.* **14**:376-85.
- Einstein DR, Kunzelman KS, Reinhall PG, Nicosia MA, Cochran RP. 2005b The relationship of normal and abnormal microstructural proliferation to the mitral valve closure sound. *J. Biomech. Eng.* **127**:134-47.
- Flachskampf FA, Chandra S, Gaddipatti A, Levine RA, Weyman AE, Ameling W, Hanrath P, Thomas JD. 2000 Analysis of shape and motion of the mitral annulus in subjects with and without cardiomyopathy by echocardiographic 3-dimensional reconstruction. *J. Am. Soc. Echocardiogr.* **13**:277-87.
- Fyrenius A, Engvall J, Janerot-Sjoberg B. 2001 Major and minor axes of the normal mitral annulus. *J. Heart Valve Dis.* **10**:146-52.
- Goetz WA, Lim HS, Pekar F, Saber HA, Weber PA, Lansac E, Birnbaum DE, Duran CMG. 2003 Anterior Mitral Leaflet Mobility Is Limited by the Basal Stay Chords. *Circulation* **107**:2969-2974.
- Hashim SR, Fontaine A, Shengqui H, Levine RA, Yoganathan AJ 1997 A three-component force vector cell for in vitro quantification of force exerted by the papillary muscle on the left ventricular wall. *J. Biomech.* **30**:1071-1075.
- Jensen KT, Fontaine A, Yoganathan AP 2001 Improved in vitro quantification of the force exerted by the papillary muscle on the left ventricular wall: three-dimensional force vector measurement system. *Ann. Biomed. Eng.* **29**:406-413.
- Jimenez JH, Soerensen DD, He Z, Ritchie J, Yoganathan AP. 2005 Mitral valve function and chordal force distribution using a flexible annulus model: an in vitro study. *Ann Biomed Eng.* 2005 **33**:557-566.
- Kunzelman KS, Einstein DR, Cochran RP. Fluid-structure interaction models of the mitral valve: function in normal and pathological states. 2007 *Philos. Trans. R. Soc. Lond. B Biol. Sci.* **362**:1393-1406.
- Kunzelman KS, Quick DW, Cochran RP. 1998a Altered collagen concentration in mitral valve leaflets: biochemical and finite element analysis. *Ann. Thorac Surg.* **66**(6 Suppl):S198-205.
- Kunzelman KS, Reimink MS, Cochran RP. 1998b Flexible versus rigid ring annuloplasty for mitral valve annular dilatation: a finite element model. *J. Heart Valve Dis.* **7**:108-116.
- Kunzelman KS, Reimink MS, Cochran RP. 1997 Annular dilatation increases stress in the mitral valve and delays coaptation: a finite element computer model. *Cardiovasc. Surg.* **5**:427-434.

- Kunzelman KS, Cochran RP, Verrier ED, Eberhart RC. 1994 Anatomic basis for mitral valve modelling. *J. Heart Valve Dis.* **3**:491-496.
- Kunzelman KS, Cochran RP, Chuong C, Ring WS, Verrier ED, Eberhart RD. Finite element analysis of the mitral valve. *J. Heart Valve Dis.* 1993a **2**:326-340.
- Kunzelman KS, Cochran RP, Murphree SS, Ring WS, Verrier ED, Eberhart RC. 1993b Differential collagen distribution in the mitral valve and its influence on biomechanical behaviour. *J. Heart Valve Dis.* **2**:236-244.
- Kunzelman KS, Cochran RP. 1990 Mechanical properties of basal and marginal mitral valve chordae tendineae. *ASAIO Trans.* **36**:M405-M408.
- Lim KH, Yeo JH, Duran CM. 2005 Three-dimensional asymmetrical modeling of the mitral valve: a finite element study with dynamic boundaries. *J. Heart Valve Dis.* **14**:386-392.
- Maisano F, Redaelli A, Soncini M, Votta E, Arcobasso L, Alfieri O. 2005 An annular prosthesis for the treatment of functional mitral regurgitation: finite element model analysis of a dog bone-shaped ring prosthesis. *Ann. Thorac. Surg.* **79**:1268-1275.
- May-Newman K, Yin FC. 1995 Biaxial mechanical behavior of excised porcine mitral valve leaflets. *Am. J. Physiol.* **269**(4 Pt 2):H1319-H1327.
- Millington-Sanders C, Meir A, Lawrence L, Stolinski C. 1998 Structure of chordae tendineae in the left ventricle of the human heart. *J. Anat.* **192**:573-581.
- Obadia JF, Casali C, Chassignolle JF, Janier M. 1997 Mitral subvalvular apparatus: different functions of primary and secondary chordae. *Circulation* **96**:3124–3128.
- Ormiston JA, Shah PM, Tei C, Wong M. 1981 Size and motion of the mitral annulus in man. I. A 2-D echocardiographic method and findings in normal subjects, *Circulation* **64**:113-120.
- Prot V, Skallerud B, Holzapfel GA. 2007 Transversely isotropic membrane shells with application to mitral valve mechanics. Constitutive modelling and finite element implementation. *Int. J. Numer. Meth. Engng.* **71**:987–1008.
- Reimink MS, Kunzelman KS, Cochran RP. 1996 The effect of chordal replacement suture length on function and stresses in repaired mitral valves: a finite element study. *J. Heart Valve Dis.* **5**:365-375.
- Reimink MS, Kunzelman KS, Verrier ED, Cochran RP. 1995 The effect of anterior chordal replacement on mitral valve function and stresses. A finite element study. *ASAIO J.* **41**:M754-M762.

- Timek TA, Nielsen SL, Green GR, Dagum P, Bolger AF, Daughters GT, Hasenkam JM, Ingels NB Jr, Miller DC. 2001 Influence of anterior mitral leaflet second-order chordae on leaflet dynamics and valve competence. *Ann. Thorac. Surg.* **72**:535–540.
- Veronesi F, Corsi C, Sugeng L, Caiani EG, Weinert L, Mor-Avi V, Cerutti S, Lamberti C, Lang RM. 2007 Quantification of Mitral Apparatus Dynamics in Functional and Ischemic Mitral Regurgitation Using Real-time 3-Dimensional Echocardiography. *J. Am. Soc. Echocardiogr.* Ahead of print (DOI:10.1016/j.echo.2007.06.017)
- Votta E, Maisano F, Bolling SF, Alfieri O, Montecvecchi FM, Redaelli A. 2007 The Geoform disease-specific annuloplasty system: a finite element study. *Ann. Thorac. Surg.* **84**:92-101.
- Votta E, Maisano F, Soncini M, Redaelli A, Montecvecchi FM, Alfieri O. 2002 3-D computational analysis of the stress distribution on the leaflets after edge-to-edge repair of mitral regurgitation. *J. Heart Valve Dis.* **11**:810-822.

CAPTIONS

Figure 1 – Section of the left heart by the valvular plane, where the mitral valve substructures can be seen.

Figure 2 – Qualitative sketches of the annular profile (left) and leaflets free margin profile (right) adopted in the computational studies from the literature. Leaflets free margin appears as if the leaflets would be excised and positioned on a planar surface.

Figure 3 – Geometrical model of the valve in its initial, end-diastolic configuration (a) obtained using echocardiographic data to define the annular profile (b), PMs initial position (c) and initial leaflets orientation (d) .

Figure 4 – Sequence of six valve configurations through the closure process, as seen from an atrial view.

Figure 5 – Maximum principal stresses acting on the leaflets during valve closure for increasing values of the trans-mitral pressure drop.

Figure 6 – Reaction forces at PMs vs time. Filled circles represent data corresponding to the antro-lateral PM; empty squares represent data corresponding to the postero-medial one.

Short title: mitral valve computational modelling in clinics

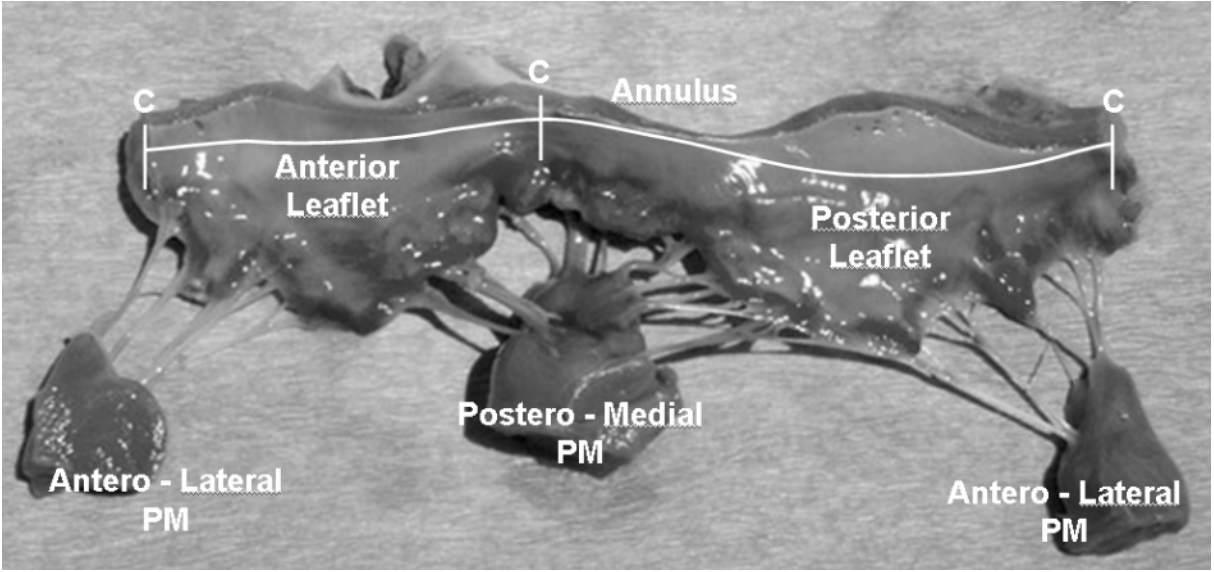


FIGURE 1





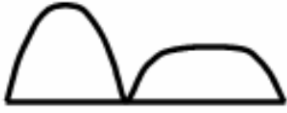
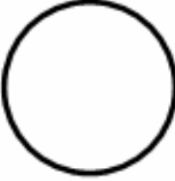
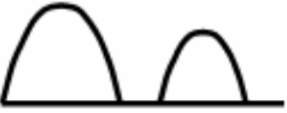
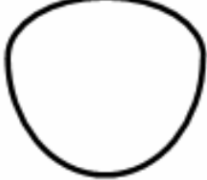

MODEL	ANNULAR PROFILE	LEAFLETS PROFILE
Kunzelman & Einstein		
Lim	REAL PROFILE	
Dal Pan		
Prot		
Votta		

FIGURE 2

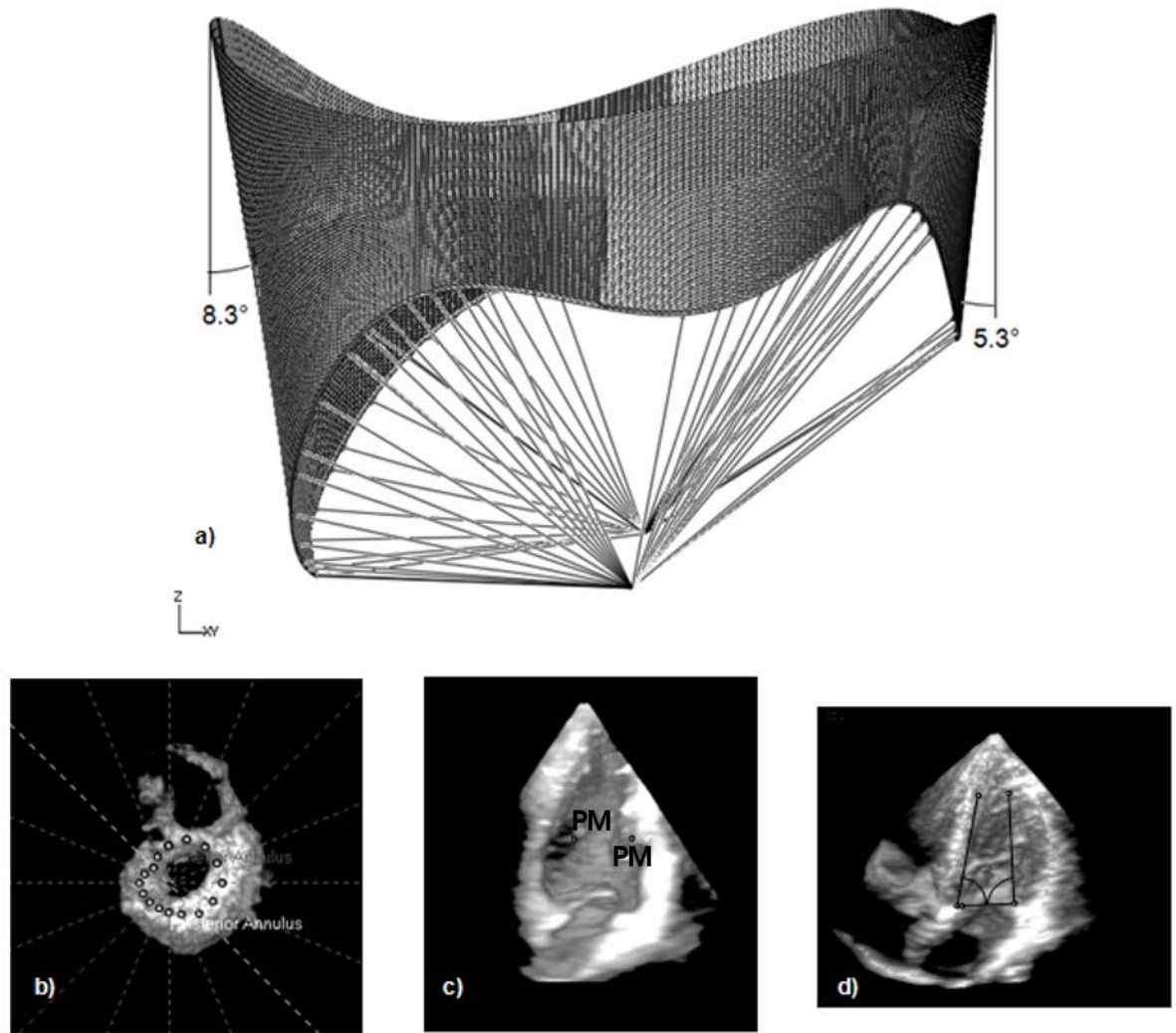


FIGURE 3

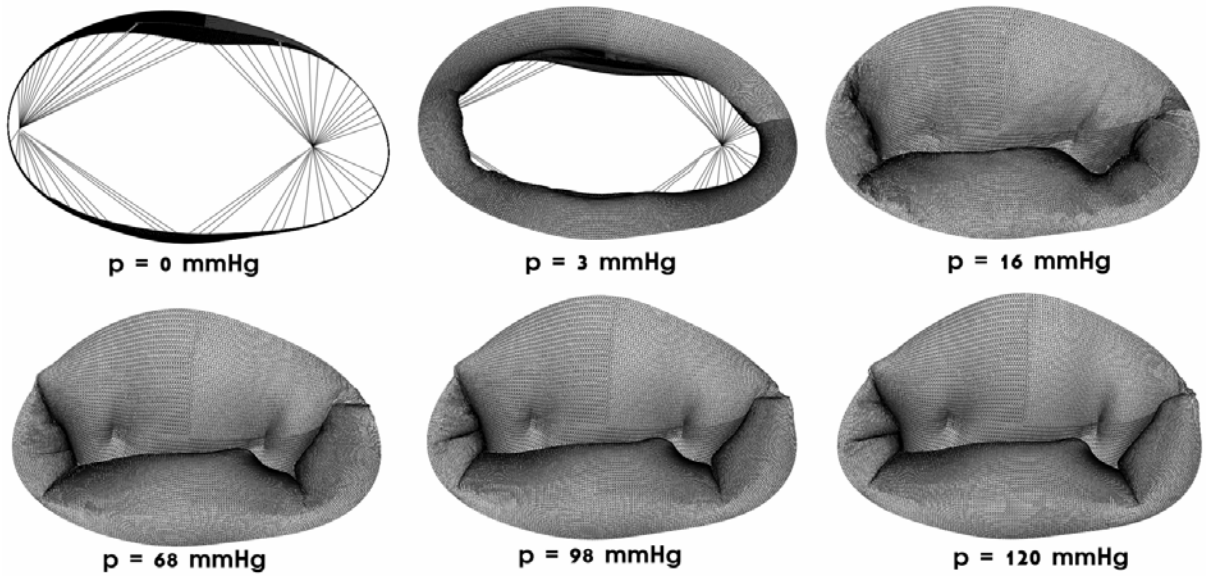


FIGURE 4

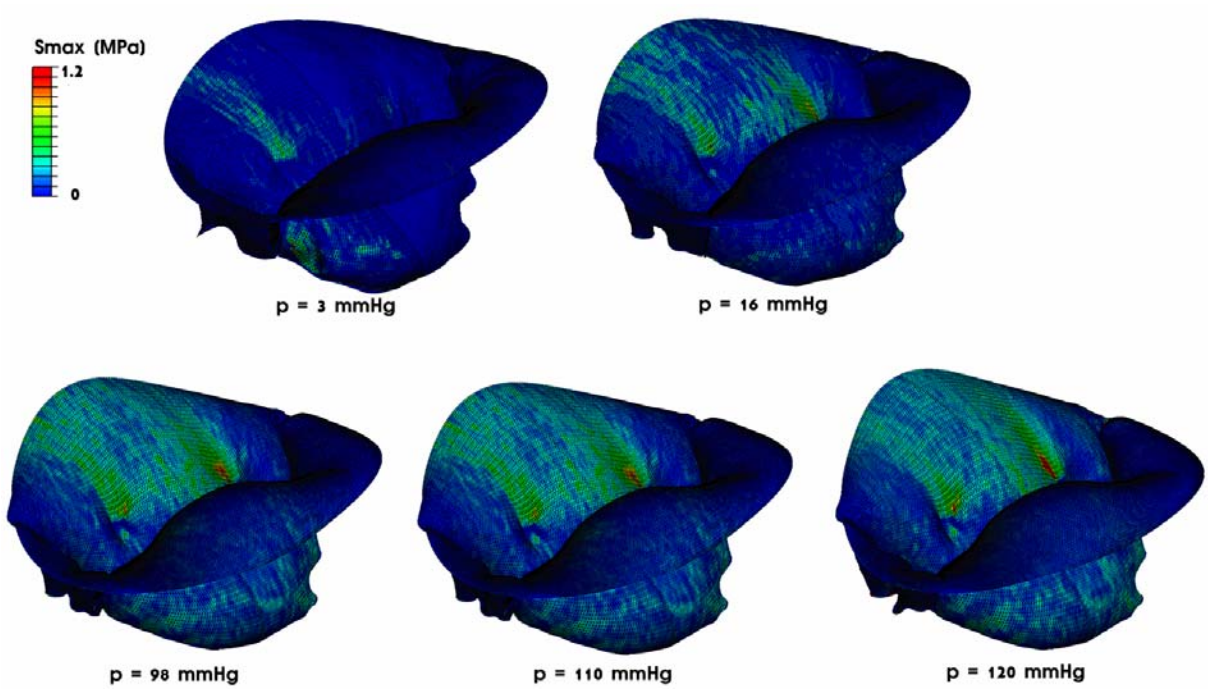


FIGURE 5

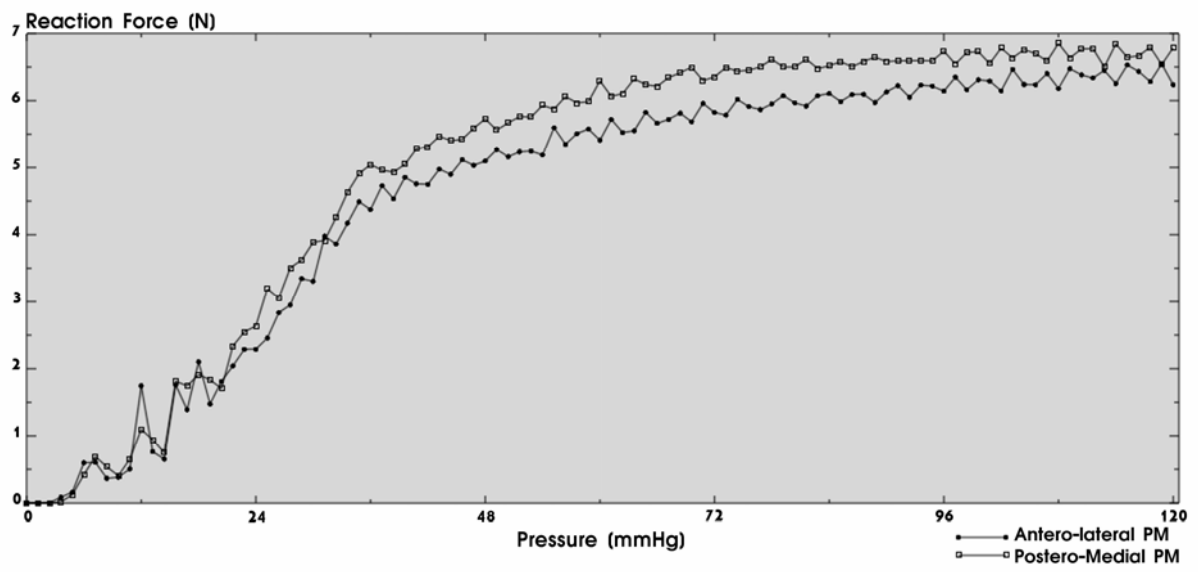


FIGURE 6